ChemPubSoc Europe

DOI: 10.1002/chem.201504103

CHEMISTRY A European Journal Full Paper

Microscopy |*Very Important Paper*|

VIP Structural Control of Cell Permeability with Highly Emissive Europium(III) Complexes Permits Different Microscopy Applications

Matthieu Starck, Robert Pal, and David Parker*[a]

Abstract: Four anionic europium complexes are described based on triazacyclononane tris-carboxylate or phosphinate ligands. In each case, the three sensitising chromophores comprise a substituted aryl–alkynyl pyridine group, with complex brightness in water falling in the range 4 to 23 $mM^{-1}cm^{-1}$. *para*-Substitution of the aryl ring with carboxymethyl groups gives complexes that are taken into cells, stain the lysosomes selectively and unexpectedly permit lifetime measurements of lysosomal pH. In contrast, the introduction of sulfonate groups inhibits cell uptake enabling the Eu complex to be used as an extracellular donor for FRET applications at the membrane surface. Using time-gated FRET microscopy, the cell membrane structure was highlighted, in which Cell Mask Deep Red was used as a membrane-localized FRET acceptor.

Introduction

We have developed a set of four europium(III) complexes, $[Eu{\cdot}L^{1-4}]^{3-}$, with very high luminescence brightness, in which remote sulfonate groups are introduced to suppress non-specific cell uptake. The precursor carboxylate complexes, in contrast, enter cells and localise to the lysosomes. Rather surprisingly, these complexes can act as lysosomal pH sensors, based on Eu lifetime modulation.

Coordination complexes of the f block elements have found diverse applications in the biological and materials sciences.[1–3] Many of these applications harness the unique properties of f-element spectroscopy. The large pseudo-Stokes' shifts, following indirect ligand excitation, and sharp emission bands allow selective detection in biological media.[4] Their long excited-state lifetimes permit time-resolved luminescence detection. Such spectral and temporal resolution engenders high signal-to-noise ratios in data acquisition, a crucial issue in imaging. In this context, many complexes of europium and terbium(III) have been developed as luminescent probes, for one or two-photon cell imaging,[5–7] as responsive probes, for example, for pH, metal ions, bicarbonate, citrate and urate measured in vitro or *in cellulo*[8–11] and as long-lived, emissive tags for FRET assays.[12]

Numerous complexes have been designed that strive to meet a set of stringent requirements for use as cellular stains, responsive probes or emissive tags: the complexes should possess high kinetic stability in biological media with respect to premature metal dissociation; they should be water soluble and resist vibrational deactivation by bound or proximate OH and NH oscillators; they should possess a high overall brightness B ($B = \varepsilon{\cdot}\Phi$) to allow detection at low concentration and, finally, they should be excited at a wavelength above about 340 nm, to avoid the use of expensive quartz optics.

The selection of the ligand and the sensitising moiety should be made with these criteria in mind. A wide variety of lanthanide coordination complexes has been studied for this purpose, including cryptates,[13] helicates,[14] polyaminocarboxylates and aminophosphinates,[15–17] notably those based on a 9-N_3 or 12-N_4 ligand framework.[18–20]

With the known high stability of lanthanide complexes of triazacyclononane-*tris*-pyridines in mind,[21] a family of europium (III) complexes (EuroTracker dyes) with exceptional brightness has been created.[22] They have been used to image certain cell organelles selectively, serve as FRET donors and tags in bioassays[23] and have been modified to function as intracellular pH probes.[23] Their exceptional brightness can be attributed to the very high extinction coefficient associated with the ICT transition,[24] the efficient intramolecular energy transfer process and effective shielding of the bound Eu^{III} ion from vibrational deactivation.[15,18d]

Herein, we report the preparation of a set of four Eu^{III} complexes (Scheme 1), investigate their photophysical properties and devise applications for each type of complex, both within and outside a living cell.

[a] *Dr. M. Starck, Dr. R. Pal, Prof. D. Parker*
Department of Chemistry
Durham University
South Road, Durham, DH1 3LE (UK)
E-mail: david.parker@dur.ac.uk

Supporting information and ORCID(s) from the author(s) for this article are available on the WWW under http://dx.doi.org/10.1002/chem.201504103.

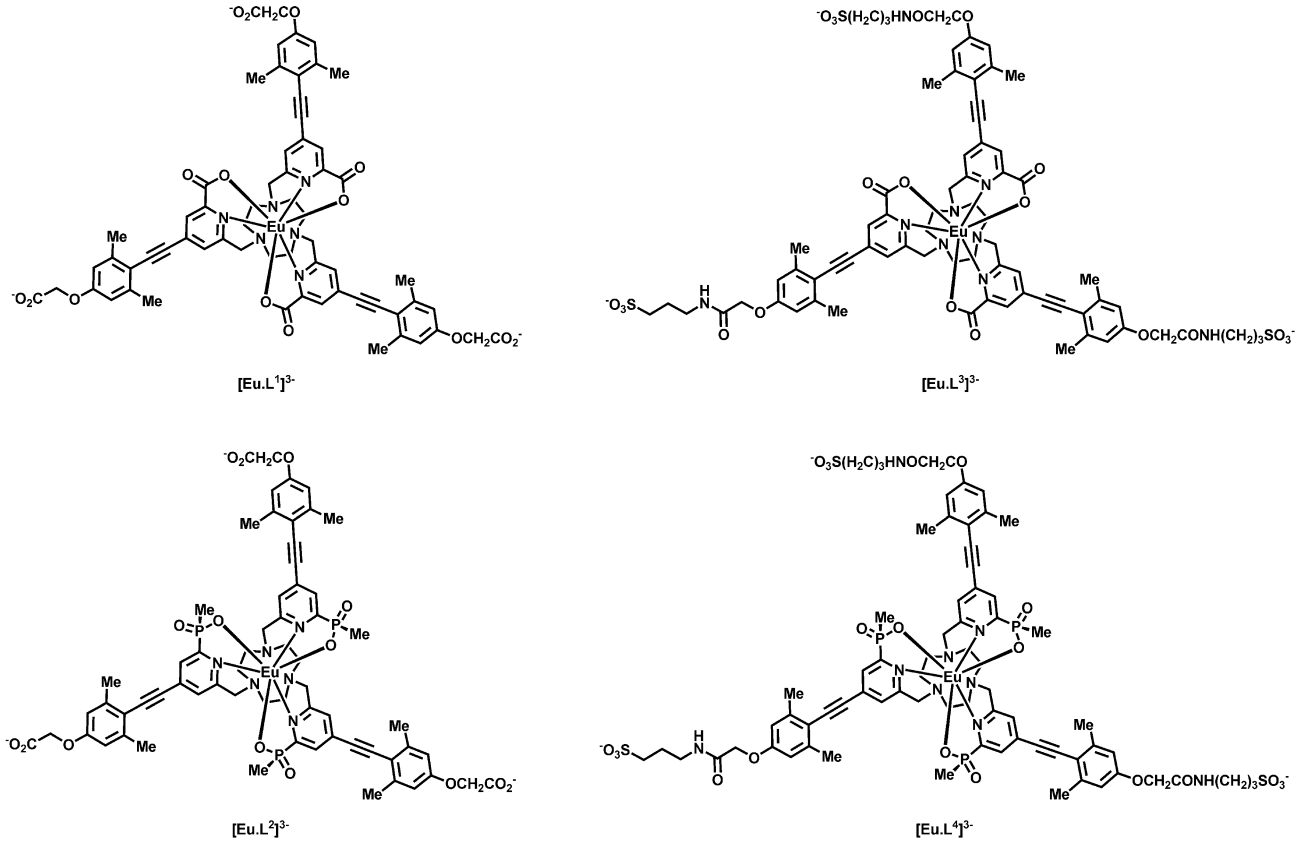

Scheme 1. Structures of the europium(III) complexes studied, $[Eu{\cdot}L^{1-4}]^{3-}$.

Results and Discussion

Synthesis

The synthesis of the tricarboxylate complex, $[Eu{\cdot}L^{1}]^{3-}$ (Scheme 2) began with commercially available aromatic and heterocyclic precursors, and used standard methodology.[22] The starting material, **1**, was prepared by alkylation of the corresponding *p*-iodophenol. Two Sonogashira palladium cross-coupling reactions were used to prepare the chromophore intermediate, **6**.

The benzylic alcohol, **6**, was converted to the corresponding mesylate **7**, which was used to alkylate 1,4,7-triazacyclononane in acetonitrile, in the presence of potassium carbonate. Near quantitative conversion afforded the ligand, **8**, which was hydrolysed in base and its europium(III) complex formed following addition of europium trichloride hexahydrate at neutral pH. The Eu^{III} complex was isolated after purification by preparative HPLC.

The synthesis of the analogous phosphinate complex (Scheme 3) involved preparation of the *p*-bromopyridyl phosphinate intermediate **9**,[22] which was elaborated to the conjugated alkynyl chromophore **10** by using a Sonogashira reaction. Subsequent mesylation of the alcohol and alkylation of triazacyclononane gave the trisubstituted macrocycle, **12**. Base hydrolysis removed all of the ethyl ester groups, after which the Eu^{III} ion was introduced and the complex purified by reverse-phase HPLC. The sulfonated derivative, $[Eu{\cdot}L^{4}]^{3-}$, was prepared by a coupling reaction using HATU (Scheme 4); similarly, the carboxylate complex analogue, $[Eu{\cdot}L^{3}]^{3-}$, was prepared and was also isolated as its ammonium salt.

Photophysical properties of the europium(III) complexes

Measurements of the photophysical properties of the four Eu^{III} complexes were performed in dilute aqueous and methanol solutions; representative data are reported in Table 1. Each complex possesses a broad absorption band around 345 nm, assigned to an intra-ligand charge-transfer transition (ICT), from the electron-donating group on the aryl ring to the electron-poor coordinated pyridine fragment. As observed in

Table 1. Spectroscopic properties of europium complexes (295 K, water; MeOH data in parentheses).

Complex	λ_{max} [nm]	ε [$mM^{-1}cm^{-1}$]	$\phi^{[a,b]}$ [%]	τ [ms][c]
$[Eu{\cdot}L^{1}]^{3-}$	348	65.0	6 (42)	0.50 (0.75)
$[Eu{\cdot}L^{2}]^{3-}$	340	67.1	16 (52)	0.81 (1.25)
$[Eu{\cdot}L^{3}]^{3-}$	348	65.1	31 (52)	0.65 (1.02)
$[Eu{\cdot}L^{4}]^{3-}$	340	67.0	34 (76)	1.07 (1.34)

[a] Quinine sulfate was used as a standard;excitation at 335 nm; errors on quantum yield or lifetime are +/−15%. [b] Errors are +/−20%. [c] In each case lifetimes in D_2O were longer than in water and consistent with the absence of a coordinated water molecule (see the Experimental Section).

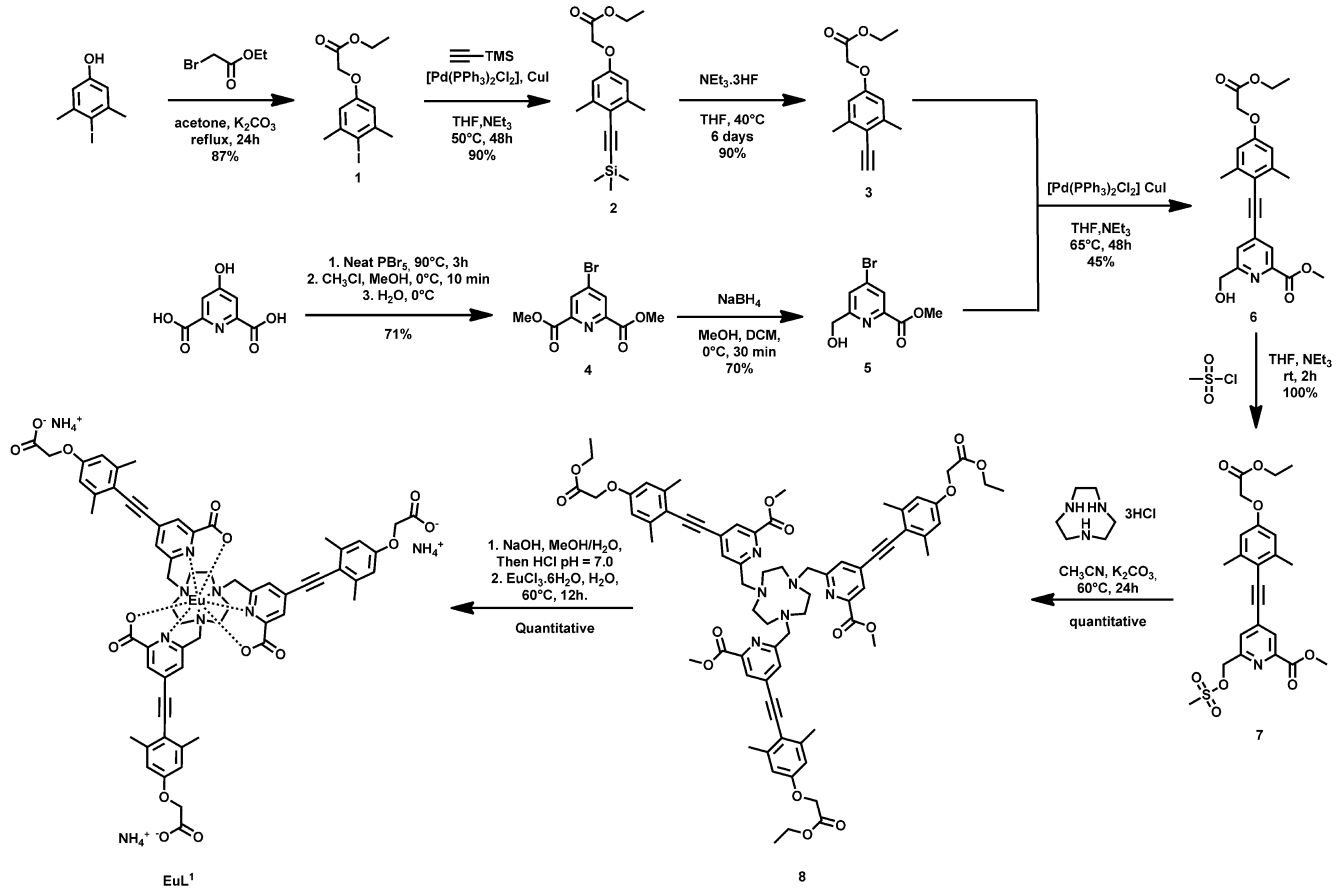

Scheme 2. Synthesis of the europium tricarboxylate complex, $[Eu{\cdot}L^{1}]^{3-}$. dppf = 1,1′-bis(diphenylphosphino)ferrocene.

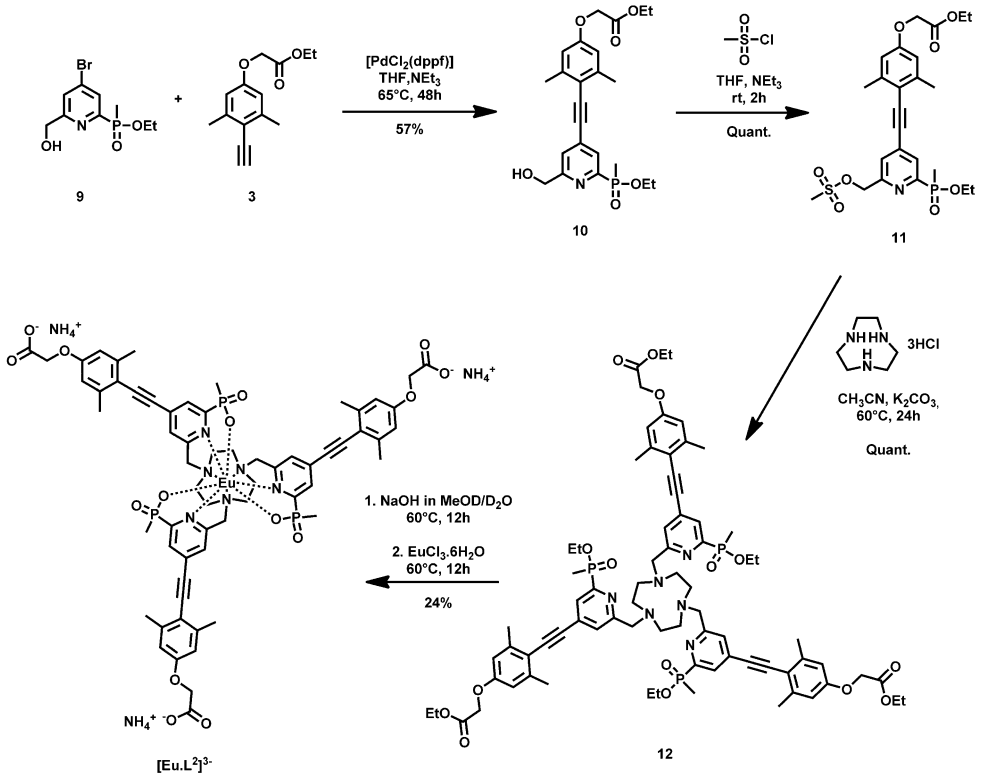

Scheme 3. Synthesis of the europium phosphinate complex, $[Eu{\cdot}L^{2}]^{3-}$.

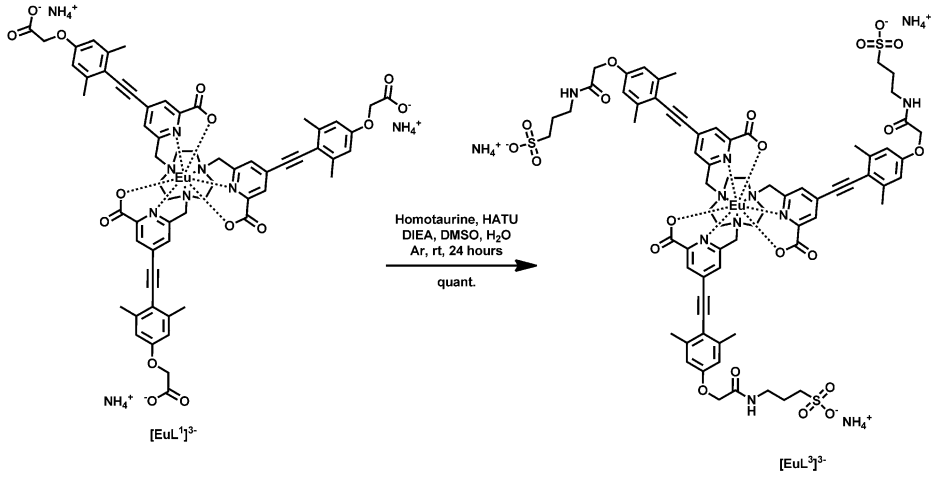

Scheme 4. Formation of the tris-sulfonate complex, $[Eu{\cdot}L^4]^{3-}$. HATU = 1-[bis(dimethylamino)methylene]-1*H*-1,2,3-triazolo[4,5-b]pyridinium 3-oxide hexafluorophosphate; DIEA = diisopropylethylamine.

recent work,[18d] the carboxylate complex absorption was slightly redshifted with respect to the phosphinate analogue, in terms of both the maximal absorption wavelength ($\Delta\lambda_{max}$ = 8 nm) and the position of the red tail of the absorption band ($\Delta\lambda_{cut\text{-}off}$ = 15 nm, Figure 1). This bathochromic shift had earlier been tentatively ascribed to a shorter Ln–N_{py} distance for the carboxylate complex, supported by comparative DFT calculations. The slightly shorter distance is indicative of stronger coordination to the europium ion, the Lewis acidity of which enhances the accepting character of the pyridine moiety.

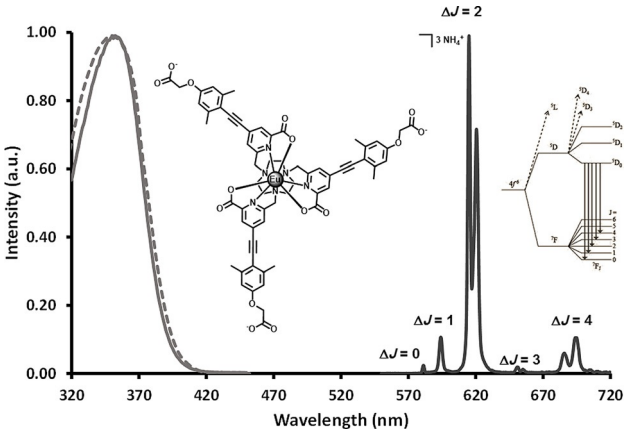

Figure 1. Absorption (dotted), excitation (left) and emission spectra (right) of $[Eu{\cdot}L^1]^{3-}$ (295 K, H_2O).

The emission spectral profiles of the four complexes were very similar (Figure 1 and ESI), with an intense hypersensitive $\Delta J = 2$ transition around 610–620 nm, as expected for such symmetric complexes incorporating polarisable donor pyridyl groups. Each complex exhibits a high quantum yield efficiency in MeOH (42 to 76%), with the highest value for the *tris*-phosphinate, $[Eu{\cdot}L^4]^{3-}$, bearing remote sulfonate groups. In water, the quantum yields and excited-state lifetimes are systematically lower, especially for the carboxylate bound complexes. Such behaviour reflects both the increased steric protection afforded by the methyl substituents at phosphorus—affecting deactivation of the Eu excited state—and the sensitivity of the energy of the ICT excited state to solvent polarity that influences the rate of intramolecular energy transfer.[18d,24] In every case, no ligand-centred emission was observed, consistent with efficient energy transfer to the lanthanide ion, and the emission lifetimes and intensities were the same in aerated and degassed solutions. The quantum yields in methanol are particularly high; the highest value (76%) was for $[Eu{\cdot}L^4]^{3-}$ and is associated with the longest luminescence lifetime of 1.34 ms. The quantum yield (34%) and lifetime (1.07 ms) in water are rather lower than in methanol and are consistent with the properties of related systems recently examined.[22–24]

The sulfonated complexes $[Eu{\cdot}L^3]^{3-}$ and $[Eu{\cdot}L^4]^{3-}$ showed no change in emission intensity and lifetime over the pH range 4 to 8, and changes in lifetime and emission intensity following addition of bovine serum albumin were less than 10% for every complex. The complexes with peripheral oxy-acetate groups showed a decrease in lifetime of 25% between pH 5 and 4 in 0.1 M NaCl solution (ESI) consistent with simultaneous protonation of the three carboxylate sites. The narrow range (over one pH unit, rather than three pH units for a mono-protonation equilibrium) for the observed variation is consistent with such behaviour, with an apparent pK_a of 4.46 (±0.08) (ESI). The reduction in lifetime may be tentatively ascribed to complex aggregation at lower pH, leading to quenching of the Eu excited state by exciplex formation.

Cell microscopy studies

The Eu complexes, $[Eu{\cdot}L^1]^{3-}$ and $[Eu{\cdot}L^2]^{3-}$ were incubated for 2 h in the cell growth medium with mouse skin fibroblast cells (NIH-3T3). Laser scanning confocal microscopy images revealed that the complexes had been internalised and gave rise to a punctate staining pattern (Figure 2). Parallel incubations with LysoTracker Green™, confirmed the selective lysosomal staining pattern. Repeating the same experiments with the

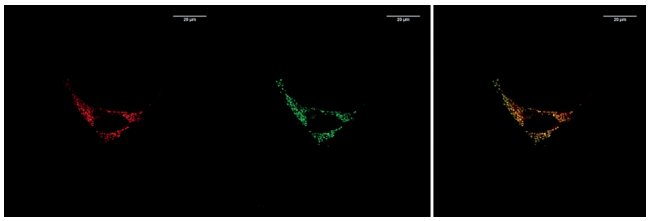

Figure 2. Confocal microscopy images of an NIH 3T3 cell following incubation with $[Eu{\cdot}L^1]^{3-}$ (10 μM, 2 h; $\lambda_{exc}=355$ nm; observe 605–720 nm) (left); LysoTracker Green (200 nM; 5 min; $\lambda_{exc}=488$ nm; observe 505–535 nm) (centre); merged image showing co-localisation ($P=0.88$; scale bar 20 μm (right) (ESI for images with and without nigericin at pH 4.6 and 6.5).

sulfonated complexes gave no staining within the cell, even after a 24 h incubation period.

The K^+/H^+ ionophore, nigericin, was added to the incubation medium (2 μM) and sequential lifetime measurements were made over the next 5 min, with excitation at 365 nm. The starting Eu lifetime was 470 μs at the 'resting' lysosomal pH; this value was assumed to be pH 4.6 (±0.1), following literature precedent.[25] At pH 6.6, the lifetime was 520 μs. The initial Eu lifetime did not change for incubations of 2, 4, 8, or 24 h, and the overall emission intensity (i.e. brightness) was also very similar at each of these time points. Such behaviour is consistent with fast, irreversible lysosomal localization, with little egress of the complex from the cell, in the absence and presence of added nigericin.

Using a LysoSensor Probe (5 μM, 5 min incubation, LSBY-DND160, λ_{exc} 355 nm), a similar experiment was undertaken, monitoring the time dependence of a neutralization process created by addition of the ionophore nigericin (2 μM). A ratio of band intensities was observed corresponding to the range 400–485 nm ('blue') versus 495–600 nm ('yellow'), (Figure 3) The final blue/yellow ratio observed was the same (±5%) as that induced by a separate addition of chloroquine (100 μM) after 4 min. Chloroquine (pK_a 10.1 and 8.4) is a lysosomotropic agent that inhibits acidification. Typically, intra-lysosomal pH values are believed to be about 6.6 (±0.1) following such treatment.[25,26]

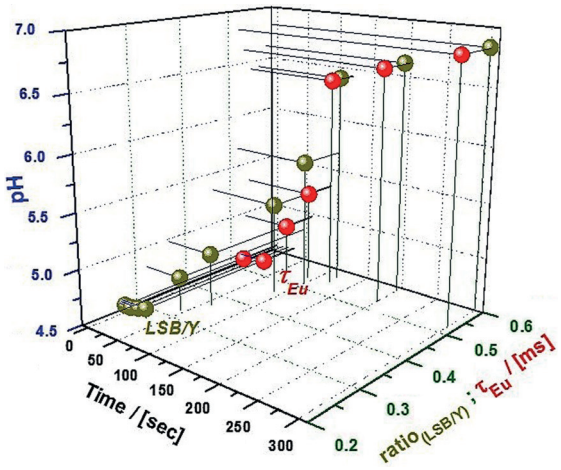

Figure 3. Variation of lysosomal pH with time, following treatment with nigericin (2 μM) in NIH-3T3 cells, monitoring Eu lifetime for $[Ln{\cdot}L^1]^{3-}$, or blue/yellow emission intensity ratio (LSB/Y) of the LysoSensor DND160.

This comparative study demonstrated that the variation of lysosomal pH with time can be monitored by observing the change in Eu emission lifetime. The direct comparison with data obtained under parallel conditions, using the fluorescent LysoSensor probe, lends support to the *in cellulo* calibration procedure, allowing the lifetime of the Eu probe to indicate lysosmal pH. Related studies with lanthanide complexes have used a similar approach to examine pH in the endoplasmic reticulum,[27] or in the lysosomes—in the latter case, this was done by measuring a ratio of Tb/Eu emission intensities in complexes of a common ligand.[28]

Time-resolved FRET studies

The sulfonated complexes $[Eu{\cdot}L^3]^{3-}$ and $[Eu{\cdot}L^4]^{3-}$ showed no cellular uptake and internalisation, and could be observed in the growth medium surrounding the cells by microscopy, (Figure 4). The Eu complex can serve as a FRET donor to a suitable accepting dye over a distance of up to 8 nm.[12,23a] The

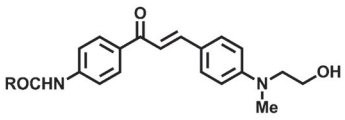

Cell Mask Deep Red ™

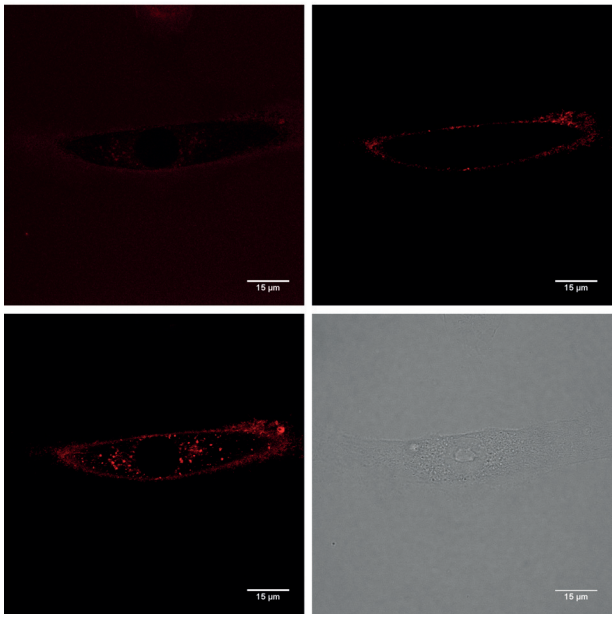

Figure 4. Laser scanning confocal microscopy images showing: the lack of internalisation of $[Eu{\cdot}L^3]^{3-}$ (internal fluorescence is due to UV induced mitochondrial autofluorescence) (1 h, 20 μM, $\lambda_{exc}=355$ nm, $\lambda_{em}=605$–635 nm) in NIH-3T3 cells pre-loaded with Cell Mask Deep Red (CMDR; 100 nM, 10 min) (top left); FRET-induced CMDR fluorescence defining only the external membrane for which FRET is possible ($\lambda_{exc}=355$ nm, $\lambda_{em}=660$–680 nm) (top right); observed CMDR fluorescence following direct excitation ($\lambda_{exc}=633$ nm, $\lambda_{em}=660$–680 nm) showing some evidence for internalisation in the punctate staining profile (lower left); cell transmission image (scale bar 15 μm, voxel size 62×62×789 nm) (lower right).[32]

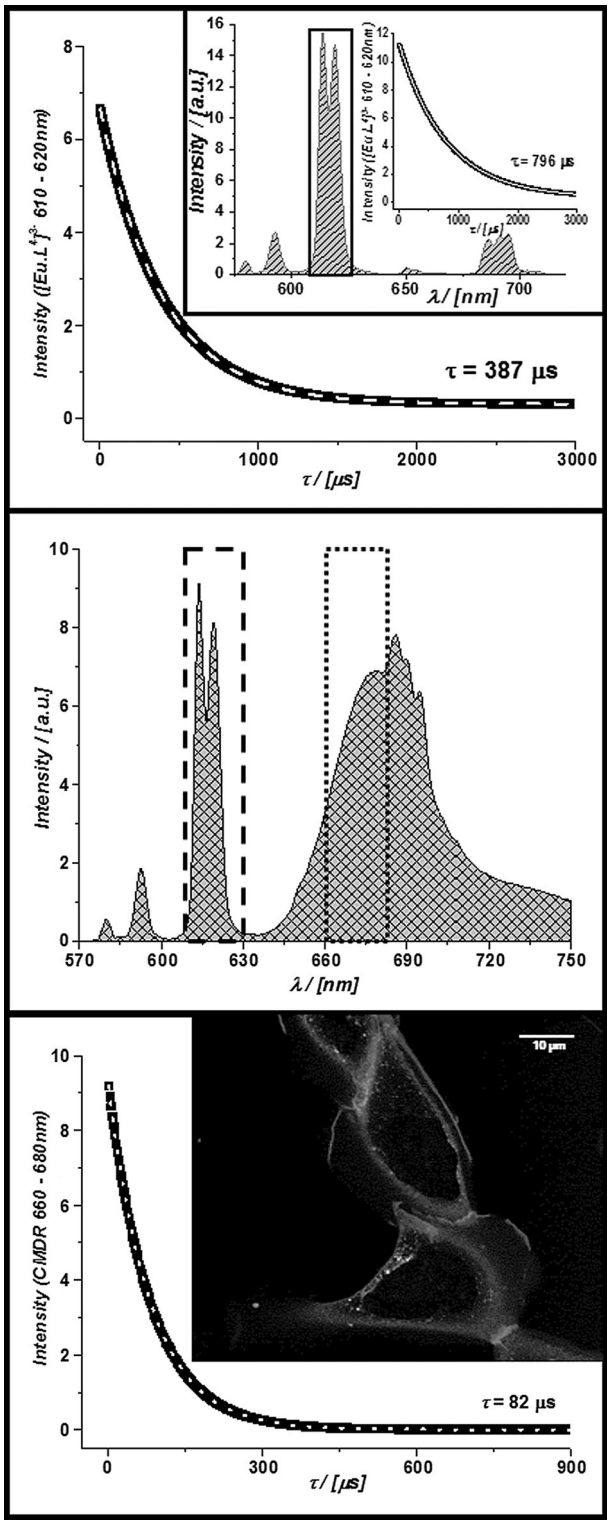

Figure 5. Reduced lifetime of $[Eu{\cdot}L^4]^{3-}$ (20 μM) when serving as a FRET donor to Cell Mask Deep Red (CMDR) (top); the insert shows the emission spectrum and corresponding lifetime of the pure Eu complex in water (λ_{exc} = 365 nm, observed at 610–630 nm); time-gated (t_g = 10 μs) spectrum of $[Eu{\cdot}L^4]^{3-}$ (20 μM) and CMDR (200 nM) (centre); enhanced lifetime of CMDR (200 nM) following FRET from the Eu donor (λ_{exc} = 365 nm, observed at 660–680 nm) (bottom). The spectra were recorded in NIH-3T3 cells (10 cells in the field of view) after 10 min pre-incubation with CMDR (washed ×3 with PBS), after loading the 'non-internalising' $[Eu{\cdot}L^4]^{3-}$ donor; the insert shows a time-gated (t_g = 10 μs) fluorescence microscopy image (scale bar 10 μ), recorded using a 250 image accumulation sequence (λ_{exc} = 365 nm, observed at 660–680 nm).[31]

membrane-staining dye, Cell Mask Deep Red (CMDR) can act as a FRET acceptor for a Eu donor in this context (Figure 5). This dye is used to stain cell membranes, but on occasion it is internalised by the cell, causing a punctate staining pattern (Figure 4, bottom left). In order to define better the membrane staining of CMDR, a time-resolved FRET microscopy study was undertaken. The lifetime of the CMDR acceptor increases dramatically under these conditions allowing the luminescence from the longer-lived dye (82 μs, Figure 5) to be observed selectively. Energy transfer between the extracellular dye and the membrane-immobilised dye acceptor can only occur in the vicinity of the membrane, so that the clarity of the FRET image is quite superior to that obtained examining dye fluorescence only, in both confocal images (Figure 4) and in a definitive time-resolved image of the membrane, using $[Eu{\cdot}L^4]^{3-}$ as the FRET donor (Figure 5, bottom).

Conclusions

The series of experiments described provide compelling evidence of the advantages to be gained by working with longer-lived emissive probes that have high inherent brightness. When a europium complex, for example, is not able to enter cells, then it can serve as a FRET donor at the membrane, allowing FRET imaging to be used to address a suitable acceptor anchored near the surface or on the membrane, to a penetration depth of about 6 to 8 nm.

The pH-dependent modulation of the lifetime of $[Eu{\cdot}L^{1,2}]^{3-}$ occurred over a narrow range in vitro, and was still observable when the probe was trapped within cellular lysosomes, thereby permitting real-time estimation of lysosomal pH in living cells. Such behaviour is of interest to those interested in examining the activity of new chemical entities in cellular models of disease, for example, for lysosomal-storage diseases, in which elevated lysosomal pH occurs.[29] Over fifty of these hereditary metabolic disorders have been described in which defective lysosomal function is found. Often, mutations in lysosomal hydrolase enzymes occur, leading to the degradation of various cellular macromolecules.[30] Therefore, time-dependent measurements of lysosomal pH using such probes, in the presence or absence of new potential drugs to treat the disease, may be of some value in the future.

Experimental Section

Optical measurements

Absorption spectroscopy: UV/Vis absorption measurements were recorded using a Perkin–Elmer Lambda 900 absorption spectrophotometer, using matched quartz cells.

Luminescence: Emission spectra were measured using a Horiba–Jobin Yvon Fluorolog-3 spectrofluorimeter. The steady-state luminescence was excited by unpolarised light from a 450 W xenon CW lamp and detected at an angle of 90° for diluted solution measurements (10 mm quartz cell) by a red-sensitive Hamamatsu R928 photomultiplier tube. Spectra were reference corrected for both

the excitation source light intensity variation (lamp and grating) and the emission spectral response (detector and grating). Phosphorescence lifetimes (>30 μs) were obtained by pulsed excitation using a FL-1040 UP Xenon Lamp. Luminescence decay curves were fitted by least-squares analysis using Origin. Luminescence quantum yields Q were measured in diluted aqueous solution with an absorbance lower than 0.1 using the following Equation (1):

$$Q_x/Q_r = [A_r(\lambda)/A_x(\lambda)][n_x^2/n_r^2][D_x/D_r] \quad (1)$$

in which A is the absorbance at the excitation wavelength (λ), n the refractive index and D the integrated luminescence intensity. "r" and "x" stand for reference and sample. Here, reference is quinine bisulfate in 1 N aqueous sulfuric acid solution ($\phi = 0.55$). Excitation of reference and sample compounds was performed at the same wavelength.

Confocal microscopy

Cell microscopy imaging of $[Eu{\cdot}L^{1-4}]^{3-}$ in cells was achieved using a custom built epiflorescence microscope (modified Zeiss Axiovert 200 M)[1], using a Zeiss APOCHROMAT 63×/1.40 NA objective, combined with a low voltage 365 nm pulsed UV LED focused and collimated excitation source (1.2 W). For rapid spectral acquisition, the microscope was equipped at the X1 port with a Peltier cooled 2D-CCD detector (Ocean Optics), used in an inverse 100 Hz time-gated sequence. The spectrum was recorded from 400–800 nm with a resolution of 0.24 nm and the final spectrum was acquired using an averaged 10000 scan duty cycle.

Probe lifetimes were measured on the same microscope platform using a novel cooled PMT detector (Hamamatsu H7155), interchangeable on the X1 port. Both the control and detection algorithm were written in LabView2011. Time-gated images were recorded using a high-resolution cooled EO-1312 M CCD camera (Thor labs). All duty cycle and gating sequences were established and controlled by in-house LabView software.[31]

High-resolution LSCM images were recorded on a modified Leica SP5 II microscope, equipped with a new SIM technique called PhMoNa.[32] In order to achieve excitation with maximal probe emission, the microscope was coupled by an optical fibre to a Coherent CW laser (Nd:YAG, 355 nm), operating at 8 mW power. A He/Ne or Ar ion laser was used when commercially available organelle-specific stains (e.g. LysoTrackerGreen) were used to corroborate cellular compartmentalization.

The microscope was equipped with a triple-channel imaging detector, comprising two conventional PMT systems and a HyD hybrid avalanche photodiode detector. The latter part of the detection system, when operated in the BrightRed mode, is capable of improving imaging sensitivity above 550 nm by 25%, reducing signal to noise by a factor of 5. The pinhole was always determined by the Airy disc size, calculated from the objective in use (HCX PL APO 63×/1.40 NA αBlue), using the lowest excitation wavelength (355 nm). Scanning speed was adjusted to 100 Hz in a unidirectional mode, to ensure both sufficient light exposure and enough time to collect the emitted light from the lanthanide-based optical probes (2048×2048 frame size, a pixel size of 62×62 nm and depth of 789 nm). Spectral imaging on this Leica system is possible with the $xy\lambda$-scan function, using the smallest allowed spectral band-pass (5 nm) and step-size (3 nm) settings. However, much improved spectral imaging in cells was achieved using a custom built and Peltier cooled CCD detector (Ocean Optics, HR2000plus) synchronized to the X1 port.

The europium complex $[Eu{\cdot}L^1]^{3-}$ (20 μM) was incubated with NIH-3T3 cells for up to 24 h to allow complex uptake within the lysosomes; this localisation profile was verified by co-incubation with LysoTracker Green. The K^+/H^+ ionophore, nigericin, was added (2 μM) and seven consecutive sets of Eu^{III} probe lifetimes were measured over the next 5 min, with excitation at 365 nm using the modified epifluorescence microscopy set up. The starting lifetime was 470 microseconds at the 'normal' lysosomal pH; this starting value was assumed to be pH 4.6 (±0.1), following literature precedent.[25] At pH 6.5, the lifetime was 520 microseconds. Replacement of the nigericin-containing medium with fresh medium led to slow restoration of the initially observed lifetime value (±10%), over a period of 1.5 h.

Using a LysoSensor Probe (5 μM, 5 min incubation, LSBYDND160, Invitrogen, $\lambda_{exc} = 355$ nm), the same experiment was performed to follow the time dependence of the increase in pH, induced by addition of the ionophore nigericin (2 μM). In this case, the ratio of band intensities observed corresponded to 400–485 nm ('blue') versus 495–600 nm ('yellow'). The final ratio measured corresponded (±5%) to that induced independently by addition of chloroquine (100 μM) after 4 min. Chloroquine ($pK_a = 10.1$ and 8.4) is an established lysosomotropic agent that accumulates in lysosomes and inhibits acidification. Typically, intra-lysosomal pH values are believed to lie in the range 6.5 to 6.7 following such a treatment.[25,26]

HPLC analysis

HPLC analysis and purifications were performed at 295 K using Shimadzu system (degassing unit DGU-20 A_{5R}, Prominence semi-preparative liquid chromatograph LC-20AP, Prominence UV/Vis detector SPD-20 A and communications bus module CBM-20A). The solvent system used was an ammonium bicarbonate buffer (25 mM, pH 7)/acetonitrile (isocratic 10% acetonitrile in buffer (3 min), linear gradient to 100% acetonitrile (10 min), isocratic 100% acetonitrile (5 min)), flow: 2 mL min^{-1} for analytical mode on XBridge C18 column, 4.6×100 mm, i.d. 5 μm, and 17 mL min^{-1} for preparative mode on XBridge C18 column, 19×100 mm, i.d. 5 μm.

Electrospray mass spectra and accurate masses

Electrospray mass spectra and accurate masses were recorded on a TQD mass spectrometer or a QTOF Premier mass spectrometer, respectively, both equipped with an Acquity UPLC, a lock-mass electrospray ion source and an Acquity photodiode array detector (Waters Ltd, UK), acetonitrile was used as the carrier solvent. The solvent system used for TQD was water (0.1% formic acid)/acetonitrile (0.1% formic acid) (5% acetonitrile (0.2 min), linear gradient to 95% Acetonitrile (3.8 min), isocratic 95% acetonitrile (0.5 min), linear gradient to 5% acetonitrile (0.5 min)), flow: 0.6 mL min^{-1} on Acquity UPLC BEH C18 column, 2.1×50 mm, i.d. 1.7 μm. The solvent system used for QTOF was ammonium bicarbonate buffer (25 mM, pH 7)/acetonitrile (2% acetonitrile in buffer (3 min), linear gradient to 40% acetonitrile (6 min), linear gradient to 100% acetonitrile (4 min), isocratic 100% acetonitrile (2 min)) or water (0.1% formic acid)/acetonitrile (0.1% formic acid) (linear gradient to 99% acetonitrile (5 min), isocratic 99% acetonitrile (1 min), linear gradient to 100% water (0.1 min), isocratic 100% water (0.9 min)), flow: 0.6 mL min^{-1} on Acquity UPLC BEH C18 column, 2.1×50 mm, i.d. 1.7 μm.

Synthesis

Details of general methods and NMR/MS instrumentation may be traced in recent references.[18d,22] Yields for final ligands and for Eu complexes were estimated by absorbance measurements of weighed samples.

Ethyl 2-(4-iodo-3,5-dimethylphenoxy)acetate (1): 4-Iodo-3,5-dimethylphenol (2.02 g, 8.06 mmol) was dissolved in acetone (10 mL). K_2CO_3 (1.46 g, 10.50 mmol) and ethyl bromoacetate (2.70 mL, 24.20 mmol) were added and the reaction was heated to reflux and stirred under argon for 24 h. The reaction was filtered to remove the potassium salts and the solvent was removed under reduced pressure. The residue was dissolved in CH_2Cl_2 (20 mL) and washed with water (20 mL). The aqueous phase was extracted into CH_2Cl_2 (3×10 mL), and combined organic layers were dried over $MgSO_4$, filtered and concentrated to dryness. The crude product was purified by flash chromatography (silica, gradient elution starting from 100% hexane to 4% EtOAc in hexane in 0.2% increments) to yield compound **1** as a white crystalline solid (2.36 g, 87%). TLC analysis: R_f: 0.25 (silica, 4% EtOAc in hexane); m.p. 79–80 °C (hexane); ^{1}H NMR (298 K, 400 MHz, $CDCl_3$):δ_H = 6.67 (2H, s), 4.58 (2H, s), 4.27 (2H, q, J = 7.0 Hz), 2.43 (6H, s), 1.30 ppm (3H, t, J = 7.0 Hz); ^{13}C NMR (298 K, 100 MHz, $CDCl_3$): δ_C = 168.9, 157.5, 143.2, 113.6, 98.5, 65.5, 61.5, 29.9, 14.3 ppm; (HRMS+): m/z: 335.0153 $[M+H]^+$ ($C_{12}H_{16}O_3{}^{127}I$ requires 335.0144); elemental analysis calculated for $C_{12}H_{15}IO_3$ (%): C = 43.13, H = 4.52, measured: C = 43.36, H = 4.52.

Ethyl 2-{3,5-dimethyl-4-[(trimethylsilyl)ethynyl]phenoxy}acetate (2): Compound **1** (500 mg, 1.5 mmol) was dissolved in anhydrous THF (5 mL) and the solution was degassed three times using consecutive freeze–pump–thaw cycles. Ethynyl trimethylsilane (7 mL, 1 M in THF, 7 mmol) and triethylamine (1 mL, 7.5 mmol) were added and the solution was degassed once more. Bis(triphenylphosphine)dichloropalladium(II) (105 mg, 0.15 mmol) and CuI (57 mg, 0.30 mmol) were added and the resulting brown solution was stirred at 55 °C under argon for 60 h. The solvent was removed under reduced pressure and the resulting brown oil was purified by column chromatography (silica, gradient elution starting from 100% hexane to 10% AcOEt in hexane in 0.2% increments) to give compound **2** as a colourless oil which solidified on standing as a white solid (410 mg, 90%). TLC analysis R_f: 0.22 (silica, 10% AcOEt in hexane); m.p. 62–63 °C (hexane); ^{1}H NMR (298 K, 400 MHz, $CDCl_3$): δ_H = 6.57 (2H, s), 4.57 (2H, s), 4.26 (2H, q, J = 7.0 Hz), 2.39 (6H, s), 1.28 (3H, t, J = 7.0 Hz), 0.25 ppm (9H, s); ^{13}C NMR (298 K, 100 MHz, $CDCl_3$): δ_C = 168.8, 157.2, 142.5, 116.6, 113.0, 102.7, 101.3, 65.2, 61.4, 21.3, 14.2, 0.3 ppm; (HRMS$^+$): m/z: 305.1574 $[M+H]^+$ ($C_{17}H_{25}O_3Si$ requires 305.1573); elemental analysis calcd (%) for $C_{17}H_{24}O_3Si$: C 67.06, H 7.88; found: C 67.03, H 7.95.

Ethyl 2-(4-ethynyl-3,5-dimethylphenoxy)acetate (3): Compound **2** (400 mg, 1.3 mmol) was dissolved in anhydrous THF (10 mL). Triethylamine trihydrofluoride (6 mL, 32 mmol) was added and the reaction was stirred at 40 °C under argon for 6 days. After this time the solvent was distilled off and the residue was purified by flash column chromatography (silica, starting from 100% hexane to 4% AcOEt in hexane) to give compound **3** as a yellow solid (272 mg, 90%). TLC analysis R_f: 0.20 (silica, 4% AcOEt in hexane); m.p. 97.5–99.5 °C (hexane); ^{1}H NMR (298 K, 400 MHz, $CDCl_3$): δ_H = 6.59 (2H, s), 4.59 (2H, s), 4.27 (2H, q, J = 7.0 Hz), 3.42 (1H, s), 2.41 (6H, s), 1.30 ppm (3H, t, J = 7.0 Hz); ^{13}C NMR (298 K, 100 MHz, $CDCl_3$): δ_C = 168.9, 157.5, 143.0, 115.6, 113.2, 84.3, 81.1, 65.3, 61.5, 21.4, 14.3 ppm; (HRMS$^+$): m/z: 233.1179 $[M+H]^+$ ($C_{14}H_{17}O_3$ requires 233.1178); elemental analysis calcd (%) for $C_{14}H_{16}O_3$: C 72.39, H 6.94; found: C 72.05, H 6.97.

Compound 4: Compound **4** was prepared as described in the literature.[33]

Methyl 4-bromo-6-(hydroxymethyl)picolinate (5): Compound **4** (550 mg, 2.0 mmol) was dissolved in anhydrous CH_2Cl_2 (5 mL) and anhydrous CH_3OH (3.5 mL) under argon atmosphere. The reaction mixture was cooled down to 0 °C. $NaBH_4$ (84 mg, 2.2 mmol) was added under argon an atmosphere and the reaction was stirred at 0 °C. After complete consumption of compound **5** (TLC monitoring), the reaction was quenched with hydrochloric acid (2 mL, 1 M). The volatile components were removed under reduced pressure and the aqueous solution was extracted into CH_2Cl_2 (20 mL). The organic layers were combined, dried over Na_2SO_4, filtered and concentrated to dryness. The crude yellowish solid was purified using flash chromatography (silica, gradient elution starting from 100% CH_2Cl_2 to 2% CH_3OH in CH_2Cl_2) to yield compound **5** (343 mg, 70%) as a white solid. TLC analysis R_f: 0.29 (silica, 3% CH_3OH in CH_2Cl_2); m.p. 131–132 °C (CH_2Cl_2); ^{1}H NMR (298 K, 400 MHz, $CDCl_3$): δ_H = 8.21 (1H, s), 7.79 (1H, s), 4.88 (2H, s), 4.03 (3H, s), 2.50 ppm (1H, br); ^{13}C NMR (298 K, 100 MHz, $CDCl_3$): δ_C = 164.6, 161.9, 148.2, 134.7, 127.4, 127.3, 64.5, 53.3 ppm; (HRMS$^+$): m/z: 245.9768 $[M+H]^+$ ($C_8H_9NO_3Br$ requires 245.9766); elemental analysis calcd (%) for $C_8H_8BrNO_3$: C 39.05, H 3.28, N 5.69; found: C 39.13, H 3.29, N 5.66.

Methyl 4-{[4-(2-ethoxy-2-oxoethoxy)-2,6-dimethylphenyl]ethynyl}-6-(hydroxymethyl)picolinate (6): Alcohol **5** (95 mg, 0.39 mmol) was dissolved in anhydrous THF (5 mL) and NEt_3 (272 μL, 1.94 mmol) was added. The reaction was degassed three times using freeze–pump–thaw. The alkyne **3** (100 mg, 0.43 mmol) was added and the solution was degassed once more. Bis(triphenylphosphine)dichloropalladium(II) (27 mg, 0.039 mmol) and CuI (15 mg, 0.078 mmol) were added and the resulting brown solution was stirred at 65 °C under argon for 36 h. The solvent was removed under reduced pressure and the resulting brown oil was purified by column chromatography (silica, gradient elution starting from 100% hexane to 10% EtOAc in hexane in 0.2% increments) to give compound **6** (66 mg, 45%) as a yellow solid. TLC analysis R_f: 0.32 (silica, 4% MeOH in CH_2Cl_2); m.p. 164–165 °C (hexane); ^{1}H NMR (298 K, 400 MHz, $CDCl_3$): δ_H = 8.08 (1H, s), 7.60 (1H, s), 6.66 (2H, s), 4.89 (2H, s), 4.65 (2H, s), 4.31 (2H, q, J = 7.0 Hz), 4.03 (3H, s), 2.50 (6H, s), 1.33 ppm (3H, t, J = 7.0 Hz); ^{13}C NMR (298 K, 100 MHz, $CDCl_3$): δ_C = 168.7, 165.4, 160.4, 158.4, 147.2, 143.2, 134.4, 125.6, 125.3, 115.1, 113.5, 93.8, 93.6, 65.3, 64.6, 61.6, 53.2, 21.5, 14.3 ppm; (HRMS$^+$): m/z: 398.1592 $[M+H]^+$ ($C_{22}H_{24}NO_6$ requires 398.1604); elemental analysis calcd (%) for $C_{22}H_{23}NO_6 \cdot 0.25\,H_2O$: C 65.74, H 5.89, N 3.48; found: C 65.85, H 5.90; N 3.30.

Methyl 4-{[4-(2-ethoxy-2-oxoethoxy)-2,6-dimethylphenyl]ethynyl}-6-{[(methylsulfonyl)oxy]methyl}picolinate (7): Alcohol **6** (43 mg, 0.11 mmol) was dissolved in dry THF (3 mL). NEt_3 (52 μL, 0.385 mmol) and methanesulfonyl chloride (12 μL, 0.16 mmol) were added. The reaction mixture was stirred at rt for 2 h and monitored by TLC. The solvent was removed under reduced pressure and the residue dissolved in CH_2Cl_2 (20 mL) and brine (10 mL). The aqueous layer was extracted with CH_2Cl_2 (3×10 mL). The combined organic layers were dried over $MgSO_4$, filtered and concentrated to dryness to yield the mesylate **7** as a yellow solid (52 mg, quantitative), which was directly used in the next step without further purification. ^{1}H NMR (298 K, 400 MHz, $CDCl_3$): δ_H = 8.14 (1H, s),

7.69 (1H, s), 6.66 (2H, s), 5.43 (2H, s), 4.64 (2H, s), 4.31 (2H, q, $J=7.0$ Hz), 4.03 (3H, s), 3.18 (3H, s), 2.50 (6H, s), 1.33 ppm (3H, t, $J=7.0$ Hz); LCMS: *m/z*: 475.9 (100% $[M+H]^+$).

Europium complex of 2,2′,2″-{[({6,6′,6″-[(1,4,7-triazacyclononane-1,4,7-triyl)tris(methylene)]tris(2-carboxypyridine-6,4-diyl)}tris-(ethyne-2,1-diyl))tris(3,5-dimethylbenzene-4,1-diyl)]tris(oxy)}triacetate [EuL^1]: 1,4,7-Triazacyclononane trihydrochloride (8 mg, 0.034 mmol) and mesylate 7 (52 mg, 0.110 mmol) were dissolved in anhydrous CH_3CN (2 mL), and K_2CO_3 (28 mg, 0.204 mmol) was added. The mixture was stirred under argon at 60 °C for 12 h. Excess potassium salts were filtered off and the filtrate was concentrated to dryness. The residue was dissolved in CH_2Cl_2 (20 mL) and H_2O (10 mL), and the aqueous layer was extracted with CH_2Cl_2 (3× 10 mL). Combined organic layers were dried over $MgSO_4$, filtered and concentrated to yield the ligand precursor **8** as a white powder residue. The residue was dissolved in a solution of MeOH/H_2O, and NaOH (30 mg, 0.75 mmol) was added to reach pH 12. The solution was heated at 60 °C overnight and hydrolysis of the ester groups monitored by LCMS and ^{1}H NMR spectroscopy. After completion, MeOH was removed under reduced pressure and the pH was adjusted to 7 by addition of a 1 M HCl solution. Then $EuCl_3{\cdot}6H_20$ (9.5 mg, 26 μmol) was added and the solution was stirred at 60 °C for 12 h. The solution was evaporated and the residue was dissolved in MeOH, and sonicated. The residual solution was filtered and evaporated to yield the crude Eu^{III} complex as a yellow solid, bright red under UV light. The complex was purified by reverse-phase HPLC (ammonium bicarbonate buffer, 25 mM) to give the ammonium salt of the europium complex (30 mg) as a pale-yellow powder after freeze-drying. (HRMS$^-$): *m/z*: 1287.302 $[M-H]^-$ ($C_{63}H_{56}N_6O_{15}{}^{151}$Eu requires 1287.300); HPLC (ammonium bicarbonate buffer, 25 mM, gradient: 10–100% CH_3CN in buffer over 10 min): $t_r=6.2$ min; $\tau_{H_2O(\text{ammonium bicarbonate})}=0.50$ ms; $\tau_{D_2O}=0.58$ ms; $\tau_{MeOH}=0.75$ ms; $q=0$; $\lambda_{max}=348$ nm; $\varepsilon_{348\,nm}=65\,000\ M^{-1}cm^{-1}$; $\phi_{H_2O}=6\%$, $\phi_{MeOH}=42\%$.

Europium complex of 2,2′,2″-({[({6,6′,6″-[(1,4,7-triazacyclononane-1,4,7-triyl)tris(methylene)]tris(2-carboxypyridine-6,4-diyl)}-tris(ethyne-2,1-diyl))tris(3,5-dimethylbenzene-4,1-diyl)]tris(oxy)-triacetamido}propane-1-sulfonate [EuL^3]: Complex [EuL^1] (1.0 mg, 0.77 μmol) and homotaurine (0.65 mg, 4.65 μmol) were dissolved in DMSO (0.2 mL) and water (20 μL). HATU (2.45 mg, 4.7 μmol) and DIEA (1.5 μL, 7.7 μmol) were added to the reaction and the mixture was stirred for 24 h under argon, after which time, HPLC and LCMS showed complete conversion. Purification by HPLC gave the ammonium salt of the [EuL^3] complex as a white solid (1.1 mg, quantitative conversion). (HRMS$^-$): *m/z*: 550.1105 $\frac{[M-3H]^{3-}}{3}$ ($C_{72}H_{78}{}^{151}EuN_9O_{21}S_3$ requires 550.1153); HPLC (ammonium bicarbonate buffer, 25 mM, gradient: 10–100% CH_3CN in buffer over 10 min): $t_r=6.6$ min; $\tau_{H_2O(\text{ammonium bicarbonate})}=0.65$ ms; $\tau_{D_2O}=0.82$ ms; $\tau_{MeOH}=1.02$ ms; $q=0$; $\lambda_{max}=348$ nm; $\varepsilon_{348\,nm}=65\,000\ M^{-1}cm^{-1}$; $\phi_{H_2O}=31\%$, $\phi_{MeOH}=52\%$.

Compound 9: Compound **9** was prepared following established procedures.[18d,22]

Ethyl 2-[4-({2-[ethoxy(methyl)phosphoryl]-6-(hydroxymethyl)pyridin-4-yl}ethynyl)-3,5-dimethylphenoxy]acetate (10): Compound **9** (105 mg, 0.36 mmol) was dissolved in dry THF (1 mL) and compound **3** (95 mg, 0.41 mmol) and NEt_3 (250 μL, 1.8 mmol) were added. The reaction was degassed three times using freeze–pump–thaw. [1,1-Bis(diphenylphosphino)ferrocene]dichloropalladium(II) (30 mg, 0.036 mmol) and CuI (7 mg, 0.036 mmol) were added and the resulting brown solution was stirred at 65 °C under argon for 18 h. The solvent was removed under reduced pressure and the resulting brown solid was purified by column chromatography (silica, gradient elution starting from 100% CH_2Cl_2 to 5% MeOH in CH_2Cl_2 in 0.2% increments) to give compound **10** (91 mg, 57%) as a pale-brown solid. TLC analysis R_f. 0.33 (silica, 5% MeOH in CH_2Cl_2); m.p. 157–158 °C (CH_2Cl_2); ^{1}H NMR (298 K, 700 MHz, $CDCl_3$): $\delta_H=8.01$ (1H, s), 7.44 (1H, s), 6.61 (2H, s), 4.80 (2H, s),4.59 (2H, s), 4.26 (2H, q, $J=7.0$ Hz), 3.97 (2H, dq, $J=175.5$ Hz, 7.0 Hz), 3.63 (1H, br. s), 2.44 (6H, s), 1.77 (3H, d, $J=15.5$ Hz), 1.28 (3H, t, $J=7.0$ Hz), 1.26 ppm (3H, t, $J=7.0$ Hz); ^{13}C NMR (298 K, 175 MHz, $CDCl_3$): $\delta_C=168.7$, 160.5 (d, $J=18.0$ Hz), 158.4, 153.4 (d, $J=156.0$ Hz), 143.3, 133.5 (d, $J=10.0$ Hz), 128.1 (d, $J=22.0$ Hz), 124.1, 115.1, 113.4, 93.9, 93.6, 65.3, 64.1, 61.6, 61.3 (d, $J=5.0$ Hz), 21.5, 16.6 (d, $J=3.5$ Hz), 14.3, 13.6 ppm (d, $J=106.0$ Hz); ^{31}P{^{1}H} NMR (298 K, 162 MHz, $CDCl_3$): $\delta_P=39.52$ ppm; (HRMS$^+$): *m/z*: 446.1734 $[M+H]^+$ ($C_{23}H_{29}NO_6P$ required 446.1733); elemental analysis calcd (%) for $C_{23}H_{28}NO_6P$: C 62.02, H 6.34, N 3.14; found: C 61.99, H 6.13, N 3.18.

Ethyl 2-[4-({2-[ethoxy(methyl)phosphoryl]-6-{[(methylsulfonyl)-oxy]methyl}pyridin-4-yl}ethynyl)-3,5-dimethylphenoxy]acetate (11): Compound **10** (10 mg, 22.5 μmol) was dissolved in dry THF (1.5 mL). Methanesulfonyl chloride (2.15 μL, 33.7 μmol) and trimethylamine (11 μL, 78.7 μmol) were added and the solution was stirred under argon at room temperature for 2 h. Solvents were

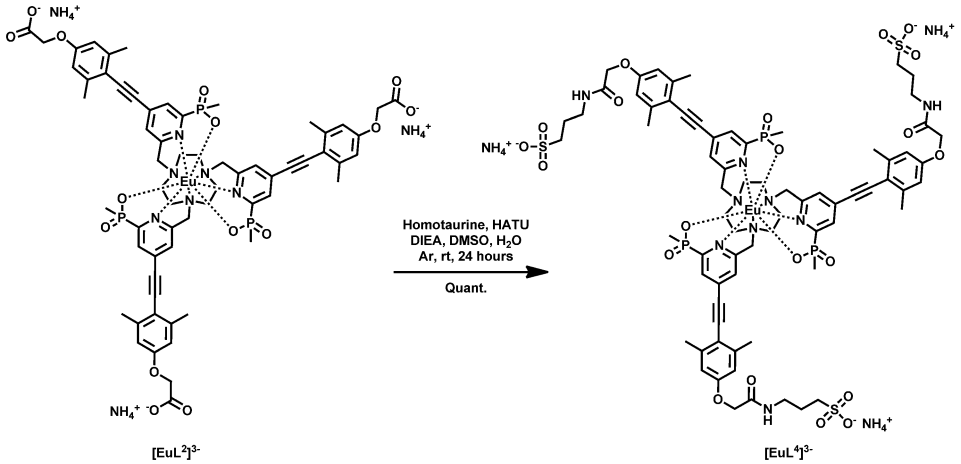

evaporated and the residue was dissolved in CH_2Cl_2 (10 mL) and brine (10 mL). The organic layer was extracted and the aqueous layer washed with CH_2Cl_2 (3×10 mL). The combined organic layers were dried over Na_2SO_4, filtered and concentrated to dryness to yield the mesylate **11** as a yellow oil (11.7 mg, quantitative), which was directly used in the next step without further purification. LCMS (ES^+ MS): *m/z*: 524.710 (100%, $[M+H]^+$).

Triethyl-2,2′,2″-[({6,6′,6″-[(1,4,7-triazacyclononane-1,4,7-triyl)-tris(methylene)]tris{2-[ethoxy(methyl)phosphoryl]pyridine-6,4-diyl})tris(ethyne-2,1-diyl)}tris(3,5-dimethylbenzene-4,1-diyl))tris-(oxy)]triacetate (12): 1,4,7-Triazacyclononane trihydrochloride (1.77 mg, 7.46 μmol) and mesylate 10 (11.7 mg, 22.5 μmol) were dissolved in anhydrous CH_3CN (0.5 mL), and K_2CO_3 (6 mg, 44.8 μmol) was added. The mixture was stirred under argon at 60 °C for 24 h. Excess potassium salts were filtered off and the filtrate was concentrated to dryness to yield a yellowish oil (10 mg, 95%) that was used directly in the next step without further purification. $^{31}P\{^1H\}$ NMR (298 K, 162 MHz, MeOD/D_2O): $\delta_P = 41.61$ ppm; LCMS (ES^+ MS): *m/z*: 1410.9 (50% $[M^+]$), 1412.2 (27%, $[M+H]^+$), 707.5 (100%, $\frac{[M-2H]^{2+}}{2}$).

Europium complex of 2,2′,2″-{[({6,6′,6″-[(1,4,7-triazacyclononane-1,4,7-triyl)tris(methylene)]tris{2-[hydroxy(methyl)phosphoryl]-pyridine-6,4-diyl}}tris(ethyne-2,1-diyl))tris(3,5-dimethylbenzene-4,1-diyl)]tris(oxy)}triacetate [EuL^2]: Compound **12** was dissolved in a solution of MeOD (1.5 mL), and a solution of NaOD in D_2O (0.5 mL, 0.1 M) was added to reach pH 12. The solution was heated at 60 °C overnight, and hydrolysis of ester groups was monitored by ^{31}P NMR. $^{31}P\{^1H\}$ NMR (298 K, 162 MHz, MeOD/D_2O): $\delta_P =$ 26.5 ppm. After completion, solvents were removed under reduced pressure and the pH was adjusted to 7 by addition of a 1 M HCl solution. $EuCl_3{\cdot}6H_20$ (2.75 mg, 7.44 μmol) was added and the solution was stirred at 60 °C for 12 h. After this time, the solution was evaporated to yield the crude Eu^{III} complex as a yellow solid, bright red under UV light. The complex was purified by HPLC in ammonium bicarbonate buffer (25 mM) to give the ammonium salt of the europium complex (2.5 mg, 24%) as a pale-yellow powder, after freeze-drying. $^{31}P\{^1H\}$ NMR (298 K, 162 MHz, MeOD): $\delta_P = +39.3$; (HRMS$^-$): *m/z*: 1397.3254 $[M-H]^-$ ($C_{63}H_{59}D_6N_6O_{15}P_3{}^{151}Eu$ requires 1397.3309); HPLC (ammonium bicarbonate buffer, 25 mM, gradient: 10–100% CH_3CN in buffer over 10 min): $t_r = 6.0$ min; $\tau_{H_2O(\text{ammonium bicarbonate})} = 0.81$ ms; $\tau_{D_2O} = 1.12$ ms; $\tau_{MeOH} = 1.25$ ms; $q = 0$; $\lambda_{max} = 340$ nm; $\varepsilon_{340\,nm} = 67\,100\ M^{-1}\,cm^{-1}$; $\phi_{H_2O} = 16\%$, $\phi_{MeOH} = 52\%$.

Europium complex of 2,2′,2″-{[({6,6′,6″-[(1,4,7-triazacyclononane-1,4,7-triyl)tris(methylene)]tris{2-[hydroxy(methyl)phosphoryl]-pyridine-6,4-diyl}}tris(ethyne-2,1-diyl))tris(3,5-dimethylbenzene-4,1-diyl)]tris(oxy)triacetamido}propane-1-sulfonate [EuL^4]: The complex $[EuL^2]$ (0.9 mg, 0.65 μmol) and homotaurine (0.55 mg, 3.90 μmol) were dissolved in DMSO (0.2 mL) and water (20 μL). HATU (2.03 mg, 3.90 μmol) and DIEA (1.26 μL, 6.50 μmol) were added to the reaction and the mixture was stirred for 24 h under argon after which time HPLC and LCMS showed complete conversion. Purification by HPLC gave the ammonium salt of the $[EuL^4]$ complex as a white solid (1.0 mg, quantitative conversion). LCMS (ES−, $C_{72}H_{81}D_6EuN_9O_{21}P_3S_3$): *m/z*: 586.130 (100%, $\frac{[M-3H]^{3-}}{3}$), 879.392 (41%, $\frac{[M-2H]^{2-}}{2}$), 1760.163 (3%, $[M-H]^-$); HPLC (ammonium bicarbonate buffer, 25 mM): $t_r = 6.3$ min; $\tau_{H_2O\ (\text{ammonium bicarbonate})} = 1.07$ ms; $\tau_{D_2O} = 1.24$ ms; $\tau_{MeOH} = 1.34$ ms; $q = 0$; $\lambda_{max} = 340$ nm; $\varepsilon_{352\,nm} = 67\,100\ M^{-1}\,cm^{-1}$; $\phi_{H_2O} = 34\%$, $\phi_{MeOH} = 76\%$.

Acknowledgements

We thank the EPSRC (MS), Royal Society and ERC for support (DP: FCC 266804).

Keywords: cell imaging · europium · luminescence FRET · microscopy

[1] C. M. Heffern, L. M. Matosziuk, T. J. Meade, *Chem. Rev.* **2014**, *114*, 4496–4539.
[2] a) S. Faulkner, S. J. A. Pope, B. P. Burton-Pye, *Appl. Spectrosc. Rev.* **2005**, *40*, 1; b) E. J. New, D. Parker, D. G. Smith, J. W. Walton, *Curr. Opin. Chem. Biol.* **2010**, *14*, 238–246; c) C. M. G. dos Santos, A. J. Harte, S. J. Quinn, T. Gunnlaugsson, *Coord. Chem. Rev.* **2008**, *252*, 2512–2527.
[3] J-C. G. Bunzli, S. V. Eliseeva, *Chem. Sci.* **2013**, *4*, 1939–1949.
[4] R. Pal, L. C. Costello, D. Parker, *Org. Biomol. Chem.* **2009**, *7*, 1525–1528.
[5] A. Picot, A. D'Aléo, P. L. Baldeck, A. Grichine, A. Duperray, C. Andraud, O. Maury, *J. Am. Chem. Soc.* **2008**, *130*, 1532–1533.
[6] a) G.-L. Law, K.-L. Wong, C. W.-Y. Man, W.-T. Wong, S.-W. Tsao, M. H.-W. Lam, P. K.-S. Lam, *J. Am. Chem. Soc.* **2008**, *130*, 3714–3715; b) F. Kielar, A. Congreve, G.-l. Law, E. J. New, D. Parker, K.-L. Wong, P. Castreno, J. de Mendoza, *Chem. Commun.* **2008**, 2435–2437; c) C. Andraud, O. Maury, *Eur. J. Inorg. Chem.* **2009**, 4357–4371.
[7] a) A. J. Palmer, S. H. Ford, S. J. Butler, T. J. Hawkins, P. J. Hussey, R. Pal, J. W. Walton, D. Parker, *RSC Adv.* **2014**, *4*, 9356–9366; b) Z. Liao, M. Tropiano, S. Faulkner, T. Vosch, T. J. Sorensen, *RSC Adv.* **2015**, *5*, 70282–70286.
[8] a) D. G. Smith, B. K. McMahon, R. Pal, D. Parker, *Chem-Eur. J.* **2012**, *18*, 11604–11613; b) Y. Bretonniere, M. J. Cann, D. Parker, R. Slater, *Org. Biomol. Chem.* **2004**, *2*, 1624–1632.
[9] R. A. Poole, F. Kielar, S. L. Richardson, P. A. Stenson, D. Parker, *Chem. Commun.* **2006**, 4084–4086.
[10] R. Pal, A. Beeby, D. Parker, *J. Pharm. Biomed. Anal.* **2011**, *56*, 352–358.
[11] B. K. McMahon, D. Parker, *RSC Adv.* **2014**, *4*, 37649–37654.
[12] a) J. M. Zwier, H. Bazin, L. Lamarque, G. Mathis, *Inorg. Chem.* **2014**, *53*, 1854–1866; b) P. Scholler, J. M. Zwier, E. Trinquet, P. Rondard, J.-P. Pin, L. Préz, *Prog. Mol. Biol. Transl. Sci.* **2013**, *113*, 275–312.
[13] a) B. Alpha, J.-M. Lehn, G. Mathis, *Angew. Chem. Int. Ed. Engl.* **1987**, *26*, 266–267; *Angew. Chem.* **1987**, *99*, 259–261; b) S. Petoud, S. M. Cohen, J.-C. G. Bünzli, K. N. Raymond, *J. Am. Chem. Soc.* **2003**, *125*, 13324–13325; c) J. D. Xu, T. M. Corneillie, E. G. Moore, G. L. Law, N. G. Butlin, K. N. Raymond, *J. Am. Chem. Soc.* **2011**, *133*, 19900–19910.
[14] a) E. Deiters, B. Song, A.-S. Chauvin, C. D. B. Vandevyver, F. Gumy, J.-C. G. Bünzli, *Chem. Eur. J.* **2009**, *15*, 885–900; b) S. V. Eliseeva, G. Auböck, F. van Mourik, A. Cannizzo, B. Song, E. Deiters, A.-S. Chauvin, M. Chergui, J.-C. G. Bünzli, *J. Phys. Chem. B* **2010**, *114*, 2932–2937.
[15] S. J. Butler, M. Delbianco, L. Lamarque, B. K. McMahon, E. R. Neil, R. Pal, D. Parker, J. W. Walton, J. M. Zwier, *Dalton Trans.* **2015**, *44*, 4791–4803.
[16] a) S. Mizukami, K. Tonai, M. Kaneko, K. Kikuchi, *J. Am. Chem. Soc.* **2008**, *130*, 14376–14377; b) M. Li, P. R. Selvin, *J. Am. Chem. Soc.* **1995**, *117*, 8132–8138.
[17] a) V.-M. Mukkala, C. Sund, M. Kwiatkowski, P. Pasanen, M. Högberg, J. Kankare, H. Takalo, *Helv. Chim. Acta* **1992**, *75*, 1621–1632; b) G. Piszczek, B. P. Maliwal, I. Gryczynski, J. Dattelbaum, J. R. Lakowicz, *J. Fluoresc.* **2001**, *11*, 101–107; c) P. Kadjane, M. Starck, F. Camerel, D. Hill, N. Hildebrandt, R. Ziessel, L. J. Charbonnière, *Inorg. Chem.* **2009**, *48*, 4601–4603; d) N. N. Katia, A. Lecointre, M. Regueiro-Figueroa, C. Platas-Iglesias, L. J. Charbonnière, *Inorg. Chem.* **2011**, *50*, 1689–1697; e) M. Starck, P. Kadjane, E. Bois, B. Darbouret, A. Incamps, R. Ziessel, L. J. Charbonnière, *Chem. Eur. J.* **2011**, *17*, 9164–9179.
[18] a) J. W. Walton, A. Bourdolle, S. J. Butler, M. Soulie, M. Delbianco, B. K. McMahon, R. Pal, H. Puschmann, J. M. Zwier, L. Lamarque, O. Maury, C. Andraud, D. Parker, *Chem. Commun.* **2013**, *49*, 1600–1602; b) L. Lamarque, O. Maury, D. Parker, J. Zwier, J. W. Walton, A. Bourdolle, Cisbio Bioassays, Codolet, PCT Int. Appl., **2013**, WO 2013011236A1 20130124; c) V. Placide, D. Pitrat, A. Grichine, A. Duperray, C. Andraud, O. Maury, *Tetrahedron Lett.* **2014**, *55*, 1357–1361; d) M. Soulié, F. Latzko, E. Bourrier, F. Placide, S. J. Butler, R. Pal, J. W. Walton, P. L. Baldeck, B. Le Guen-

nic, C. Andraud, J. M. Zwier, L. Lamarque, D. Parker, O. Maury, *Chem-Eur. J.* **2014**, *20*, 8636 – 8646.
[19] S. J. Butler, D. Parker, *Chem. Soc. Rev.* **2013**, *42*, 1652 – 1666.
[20] S. Pandya, J. Yu, D. Parker, *Dalton Trans.* **2006**, 2757 – 2766.
[21] a) H. Takalo, I. Hemmilä, T. Sutela, M. Latva, *Helv. Chim. Acta* **1996**, *79*, 789 – 802; b) C. Gateau, M. Mazzanti, J. Pecaut, F. A. Dunand, L. Helm, *Dalton Trans.* **2003**, 2428 – 2433; c) G. Nocton, A. Nonat, C. Gateau, M. Mazzanti, *Helv. Chim. Acta* **2009**, *92*, 2257 – 2273.
[22] S. J. Butler, L. Lamarque, R. Pal, D. Parker, *Chem. Sci.* **2014**, *5*, 1750 – 1756.
[23] a) M. Delbianco, V. Sadovnikova, E. Bourrier, L. Lamarque, G. Mathis, D. Parker, J. M. Zwier, *Angew. Chem. Int. Ed.* **2014**, *53*, 10718 – 10722.
[24] a) A. Picot, F. Malvolti, B. Le Guennic, P. L. Baldeck, J. A. G. Williams, C. Andraud, O. Maury, *Inorg. Chem.* **2007**, *46*, 2659 – 2665; b) A. D'Aléo, A. Picot, A. Beeby, J. A. G. Williams, B. Le Guennic, C. Andraud, O. Maury, *Inorg. Chem.* **2008**, *47*, 10258 – 10268.
[25] M. O. Bevensee, E. Bashi, W. F. Boron, *J. Membr. Biol.* **1999**, *169*, 131 – 139.
[26] S. Ohkuma, B. Poole, *Proc. Natl. Acad. Sci. USA* **1978**, *75*, 3327 – 3331.
[27] B. K. McMahon, R. Pal, D. Parker, *Chem. Commun.* **2013**, *49*, 5363 – 5365.
[28] a) D. G. Smith, B. K. McMahon, R. Pal, D. Parker, *Chem. Commun.* **2012**, *48*, 8520 – 8522; b) R. Pal, D. Parker, *Org. Biomol. Chem.* **2008**, *6*, 1020 – 1033.
[29] T. Fukuda, L. Ewan, M. Bauer, R. J. Mattaliano, K. Zaal, E. Ralston, P. H. Plotz, N. Raben, *Ann. Neurol.* **2006**, *59*, 700 – 708.
[30] F. M. Platt, R. H. Lachmann, *Biochim. Biophys. Acta Mol. Cell Res.* **2009**, *1793*, 737 – 745; R. H. Lachmann, *Biochem. Soc. Trans.* **2010**, *38*, 1465 – 1468.
[31] R. Pal, A. Beeby, *Methods Appl. Fluoresc.* **2014**, *2*, 037001 – 0307007.
[32] R. Pal, *Faraday Discuss.* **2015**, *177*, 507 – 515.
[33] H. Takalo, J. Kankare, *Acta. Chem. Scand. Ser. B* **1987**, *41*, 219 – 221.

Received: October 13, 2015
Published online on December 16, 2015

